Published online February 12, 2004

1006–1017 *Nucleic Acids Research, 2004, Vol. 32, No. 3*
DOI: 10.1093/nar/gkh268

A mutation in polynucleotide phosphorylase from *Escherichia coli* impairing RNA binding and degradosome stability

Maria Elena Regonesi[1,2], Federica Briani[2], Andrea Ghetta[1], Sandro Zangrossi[3], Daniela Ghisotti[2], Paolo Tortora[1] and Gianni Dehò[2,*]

[1]Dipartimento di Biotecnologie e Bioscienze, Università degli Studi di Milano-Bicocca, Piazza della Scienza 2, 20126 Milan, Italy, [2]Dipartimento di Scienze Biomolecolari e Biotecnologie, Università degli Studi di Milano, Via Celoria 26, 20133 Milan, Italy and [3]Istituto di Biofisica, Sezione di Milano, Consiglio Nazionale delle Ricerche, Via Celoria 26, Milan, Italy

Received November 18, 2003; Revised and Accepted January 15, 2004

ABSTRACT

Polynucleotide phosphorylase (PNPase), a 3′ to 5′ exonuclease encoded by *pnp*, plays a key role in *Escherichia coli* RNA decay. The enzyme, made of three identical 711 amino acid subunits, may also be assembled in the RNA degradosome, a hetero-multimeric complex involved in RNA degradation. PNPase autogenously regulates its expression by promoting the decay of *pnp* mRNA, supposedly by binding at the 5′-untranslated leader region of an RNase III-processed form of this transcript. The KH and S1 RNA-binding domains at the C-terminus of the protein (amino acids 552–711) are thought to be involved in *pnp* mRNA recognition. Here we show that a G454D substitution in *E.coli* PNPase impairs autogenous regulation whereas it does not affect the catalytic activities of the enzyme. Although the mutation maps outside of the KH and S1 RNA-binding domains, analysis of the mutant protein revealed a defective RNA binding, thus suggesting that other determinants may be involved in PNPase–RNA interactions. The mutation also caused a looser association with the degradosome and an abnormal electrophoretic mobility in native gels. The latter feature suggests an altered structural conformation of PNPase, which may account for the properties of the mutant protein.

INTRODUCTION

Polynucleotide phosphorylase (PNPase, polyribonucleotide nucleotidyltransferase, EC 2.7.7.8) is one of the main exoribonucleolytic activities involved in RNA turnover in bacteria and chloroplasts (1,2). Recently PNPase has also been localized in human mitochondria (3) and PNPase homologues are found in metazoan sequenced genomes, but no hortologues have been so far identified in *Archaea* (www.ncbi.nlm.nih.gov). In *Escherichia coli* the protein is a homotrimer of a 711 amino acid polypeptide encoded by *pnp* (4,5). The three-dimensional crystallographic structure of the homologous protein from *Streptomyces antibioticus* (6) shows that each PNPase subunit is composed of a duplicated structural core, which contains the catalytic domain(s), an all-α-helical domain located at the bottom and two C-terminal RNA-binding domains, KH and S1 (7,8), on the top. The three subunits associate via trimerization interfaces of the core domain, forming a central channel.

In vitro, PNPase catalyses the processive 3′ to 5′ phosphorolytic degradation of RNA, the reverse reaction (i.e. the polymerization of ribonucleoside diphosphates with release of phosphate) and the exchange reaction between free phosphate and the β-phosphate of ribonucleoside diphosphates (9–12). PNPase can also bind RNA (5,10,13), supposedly via its two RNA-binding domains. *In vivo*, the enzyme has been shown to be involved in both processive phosphorolytic degradation and polyadenylation of RNAs (14,15), and may be found as a component of a multiprotein machine, the RNA degradosome, together with the endonuclease RNase E, which provides the scaffold to the entire structure, the DEAD-box RNA helicase RhlB and enolase (16,17).

Genetic and molecular studies have implicated PNPase in several cell processes, which may account for the pleiotropic effects of *pnp* mutants. PNPase does not seem to be indispensable to *E.coli* at optimal temperature, unless either RNase II or RNase R, the other main exonucleolytic activities of the cell, are defective (14,18,19). However, PNPase defective mutants cannot grow at low temperatures (e.g. 16°C) (20). PNPase autogenously regulates its own expression by promoting the instability of its mRNA (21–23). The current model of PNPase autogenous regulation maintains that the leader region of the *pnp* primary transcript forms a long stabilizing hairpin that is rapidly processed by a staggered double strand cut by RNase III. This leaves at the 5′-end of the

*To whom correspondence should be addressed. Tel: +39 02 5031 5019; Fax: +39 02 5031 5044; Email: gianni.deho@unimi.it

The authors wish it to be known that, in their opinion, the first two authors should be regarded as joint First Authors

processed *pnp* mRNA a short duplex with a 3′-extension that stabilizes the transcript unless it is removed by the phosphorolytic activity of PNPase. Both phosphorolytic and RNA-binding activities of PNPase are thought to be essential for this process (23,24). In agreement with the proposed regulatory model, both mutations that abolish PNPase enzymatic activity and those located in the RNA-binding domains impair autogenous regulation (24,25). In the cold acclimation phase, autogenous regulation is temporarily alleviated and *pnp* mRNA becomes stabilized, although PNPase expression does not increase accordingly (26–28).

In a previous work we isolated an *E.coli pnp* mutant, originally named *bfl-1*, impaired in maturation of bacteriophage P4 CI RNA, a small stable RNA responsible for the prophage super-infection immunity (29,30). In this mutant the primary transcript of the P4 immunity region became more stable and accumulated, while RNase P-mediated maturation of CI RNA was greatly delayed. Here we show that the mutation, a Gly454Asp substitution in the core region, does not affect the catalytic activity of the enzyme; rather, it appears to alter the overall conformation of the protein and to impair RNA binding, PNPase autogenous regulation and degradosome stability.

MATERIALS AND METHODS

Bacterial strains and plasmid

Escherichia coli strains C-5601 (*pnp-701*~Tn*5*), C-5602 (*pnp*$^+$~Tn*5*) and C-5612 (*pnp-7*~Tn*10*) (29) are isogenic derivative of the prototrophic *E.coli* C-1a (31) (the symbol ~ indicates P1 cotransducibility between the gene and the transposon). The *pnp-7* allele carries a nonsense (opal) mutation in codon 233 and a base substitution in the putative Shine–Dalgarno sequence of the gene (26). C-5613 (*pnp*$^+$~Tn*10*) was obtained by P1 transduction together with the isogenic C-5612, as described (29).

The following plasmids were derivatives of the low copy number vector pGZ119-HE [ColD replicon, confers chloramphenicol resistance (32)]. Coordinates of cloned *E.coli* DNA fragments and oligonucleotides are from DDBJ/EMBL/GenBank accession no. AE000397, unless otherwise indicated. pAZ8 (*pnp*$^+$; 8006–5391), pAZ12 (*pnp-701*; 8148–5339) and pAZ13 (*pnp-7*; 8148–5339) were described previously (29). pAZ101 was obtained by digestion of pAZ8 at its unique SalI site in the polylinker, filling in with Klenow, and ligation. This also destroys the AccI site in the vector, leaving a unique AccI in the cloned *pnp* fragment. pAZ130 and pAZ131 are pAZ101 derivatives carrying the Gly454Asn (*pnp-702*) and Gly454Leu (*pnp*-703) mutations, respectively. They were obtained by site-directed mutagenesis, as detailed in the following section.

The pGEM-3Z (Promega, Madison, WI) derivatives pAZ16 and pAZ410 were used as templates for *in vitro* transcription of the labelled riboprobes specific for *pnp* and *rpsO* transcripts, respectively (26).

Mutation analysis and site-directed mutagenesis

The *pnp* region was sequenced by cycle sequencing using C-5601 and C-5602 genomic DNA and the AmplyCycle sequencing kit (Perkin Elmer, Branchburg, NJ). Construction of plasmid pAZ130, which carries the *pnp-702* Gly454Asn mutation created by site-directed mutagenesis (33), was done as follows. The DNA fragments 6775–6424 and 6447–6048 of the *pnp* gene were obtained by PCR amplification of pAZ8 with the two oligonucleotide pairs 139 (6775–6756)–914 (6424–6447) and 915 (6447–6424)–733 (6048–6064). The complementary 914 and 915 oligonucleotides carried a three base substitution (ACC→GTT in 914, GGT→AAC in 915) that changed the 454Gly codon of *pnp* into an Asn codon. The DNA fragments obtained from these PCRs, which were partially overlapping, were mixed, annealed, extended and amplified in a second PCR with the external 139 and 733 oligonucleotides. The product of this amplification was digested with BsiWI and BsaBI and cloned in pAZ101 digested with the same enzymes. The resulting pAZ130 plasmid was checked by restriction analysis and sequencing of the amplified region. Construction of plasmid pAZ131, which carries the *pnp-703* Gly454Leu mutation, was done in the same way, except that oligonucleotides 1097 and 1098, which differ from 914 and 915, respectively, for the desired mutation, were used for the first PCR to obtain the GGT→CTG base substitutions at the *pnp* 454 codon.

Preparation of crude extracts

Escherichia coli cells were grown in a rotatory shaker at 37°C in 200 ml of LD medium [5 g/l DIFCO yeast extract (Becton Dickinson Microbiology Systems, Sparks, MD), 10 g/l DIFCO tryptone, 5 g/l NaCl] up to mid-exponential phase (OD_{600} = 0.8). Chloramphenicol (30 μg/ml) was added to the medium when the strains harboured a plasmid conferring antibiotic resistance. Cells were harvested, washed with 50 mM Tris–HCl pH 7.4 and stored at –20°C. Frozen cells were resuspended in 4 ml/g_{cell} of lysis buffer [50 mM Tris–HCl pH 7.4, 0.1 mM DTT, 0.5 mM EDTA, 1 mM PMSF, 5% glycerol (v/v) and Complete™ EDTA-free protease inhibitor (1 tablet/50 ml; Roche, Mannheim, Germany)] and disrupted by sonication at 0°C. After incubation with DNase I (Sigma, St Louis, MO) for 10 min at 37°C, debris was removed by centrifugation at 20 000 *g* and the supernatant dialysed at 4°C against 50 mM Tris–HCl pH 7.4, 0.1 mM DTT, 0.5 mM EDTA and 5% glycerol. Extracts were stored at –20°C in 50% glycerol.

Purification of wild-type PNPase

A crude cell extract was prepared as described above from 50 litres of a C-5602/pAZ101 culture and PNPase was purified as described (34), except that in the last step of purification the PNPase preparation was applied to a polyA–Sepharose column (Sigma) (3 ml bed volume), pre-equilibrated with 20 mM Tris–HCl pH 7.4, 10 mM $MgCl_2$, 0.1 mM DTT, 10% glycerol and Complete™ EDTA-free protease inhibitor. The column was washed, first with 5 ml of 20 mM Tris–HCl pH 8.0, 10 mM $MgCl_2$, 0.1 mM EDTA, 0.1 mM DTT, 10% glycerol and protease inhibitor, and then with 5 ml of the same buffer with 0.4 M NaCl. The enzyme was eluted with 25 ml of 20 mM Tris–HCl pH 8.0, 0.1 mM DTT, 2 M NaCl, 10% glycerol and protease inhibitor. Two-millilitre fractions were immediately concentrated in a Centricon YM-30 microconcentrator (Millipore, Bedford, MA), diluted with 50 mM Tris–HCl pH 7.4, 0.1 mM DTT, 10% glycerol, 0.1 mM EDTA and

protease inhibitor, concentrated again to a protein concentration of 4 mg/ml and stored at –20°C in 50% glycerol.

Purification of Pnp-701 protein

A crude cell extract was prepared as described above from 4 litres of a C-5601/pAZ12 culture. The non-dialysed supernatant was incubated with 0.4 mg/g_{cell} RNase A (Sigma) for 60 min at room temperature and then loaded at a flow rate of 0.5 ml/min onto a DEAE–Sephacel column (Amersham Pharmacia Biotech, Little Chalfont, Buckinghamshire, UK) (bed volume, 25 ml), pre-equilibrated with 25 mM Tris–HCl pH 8.0 and 10% glycerol. The column was washed with 5 volumes of the same buffer and the enzyme eluted with a linear 0–0.5 M NaCl gradient in the same buffer at a flow rate of 1 ml/min. Ten-millilitre fractions were collected. The fraction displaying the highest specific activity was run in native gradient gel electrophoresis (6–16% running gel). The visible band formed by PNPase was excised from the gel and ground in a Potter homogenizer in 4 ml of 20 mM Tris–HCl pH 8.0, 0.1 mM DTT and 20% glycerol. Gel debris was spun off and re-extracted with 6 ml of the same buffer. The two volumes were combined and centrifuged at 1900 *g* for 5 min, and the supernatant was concentrated in Centricon YM-30 microconcentrators (Millipore) to a final volume of 200 µl.

Degradosome purification

Purified degradosomes were prepared as described (16), with some modifications, from strains C-5602 (*pnp*$^+$) and C-5601 (*pnp-701*). Frozen cell paste (5 g) was broken by a lysozyme/freeze–thaw lysis procedure (35) in 10 ml of lysozyme–EDTA buffer [50 mM Tris–HCl pH 7.4, 100 mM NaCl, 5% glycerol, 3 mM EDTA, 1 mM DTT, 1.5 mg/ml lysozyme (Sigma), 1 mM PMSF, Complete™ EDTA-free protease inhibitor]. Five millilitres of DNase–Triton buffer [50 mM Tris–HCl pH 7.4, 100 mM NaCl, 5% glycerol, 1 mM DTT, 30 mM magnesium acetate, 3% Triton X-100, 1 mM PMSF, 20 µg/ml DNase I (Sigma), Complete™ EDTA-free protease inhibitor] was then added and the suspension incubated for 30 min at room temperature. Subsequently, 3.75 ml of 5 M NH_4Cl was slowly added with stirring at 4°C. The lysate was incubated for another 30 min and then clarified by centrifugation at 20 000 *g* for 60 min. A high-speed supernatant was prepared by centrifugation at 200 000 *g* for 2 h. The supernatant was precipitated with ammonium sulphate (40% saturation) and the pellet resuspended in 10 ml of buffer A (10 mM Tris–HCl pH 7.4, 5% glycerol, 1 mM EDTA, 0.1 mM DTT, 0.1 mM PMSF, 0.5% Genapol X-80, Complete™ EDTA-free protease inhibitor) containing 50 mM NaCl, 1 mM DTT and 1 mM PMSF. The resuspended pellet was applied to an SP-Sepharose™ High Performance column (Amersham Biosciences, UK) (bed volume, 6 ml), pre-equilibrated with buffer A containing 50 mM NaCl. The sample was applied at 0.15 ml/min and the column was washed, first with 5 volumes of equilibration buffer and then with 5 volumes of buffer A containing 300 mM NaCl. The degradosome was eluted with 3 volumes of buffer A containing 1 M NaCl and 1% Genapol X-80. Six-millilitre fractions were collected and glycerol added to a 30% final concentration.

Analysis of the degradosome by gel filtration

The first fraction obtained from SP-Sepharose chromatography was concentrated with Centricon YM-30 microconcentrators (Millipore) and subjected to a gel filtration on a Superose 6 HR 10/30 column (Amersham Biosciences), pre-equilibrated with 20 mM Tris–HCl pH 7.4, 300 mM NaCl, 1 mM EDTA, 0.1 mM PMSF, 0.1% Genapol X-80 and Complete™ EDTA-free protease inhibitor. Elution was performed at a flow rate of 0.5 ml/min in the same buffer. Fractions (0.25 ml) were collected and stored in 50% glycerol at –20°C. Apparent molecular masses were assessed based on elution volumes of suitable markers (Blue dextran 2000 kDa, thyroglobulin 669 kDa, apoferritin 443 kDa, α-amylase 200 kDa, aldolase 158 kDa, bovine serum albumin 67 kDa, ovalbumin 43 kDa).

Assays

Protein content was determined using the Coomassie® Plus Protein Assay Reagent (Pierce, Rockford, IL) and bovine plasma immunoglobin G as standard protein. Unless otherwise stated, PNPase phosphorolytic activity was determined using a photometric cyclic assay as previously reported (36). This is suitable for activity determinations in crude extracts. Alternatively, PNPase phosphorolytic activity was assayed photometrically using the method described by Godefroy (10), with minor modifications (36). Polymerase activity of PNPase was assayed by incubating pure enzyme at 37°C in 50 mM Tris–HCl pH 7.4, 0.1 M KCl, 5 mM $MgCl_2$ and 0.2 or 1 mM ADP. Samples were withdrawn at predefined times, and free phosphate determined using a colorimetric method as previously reported (37). Enolase activity was assayed photometrically as described (38) with minor modifications. The assay reveals the phospho*enol*pyruvate released by taking advantage of pyruvate kinase and lactate dehydrogenase as auxiliary enzymes. Briefly, in the assay mixture (1 ml) were present 50 mM Tris–HCl pH 7.4, 0.1 M KCl, 5 mM $MgCl_2$, 0.14 mM NADH, 1.1 mM ADP, 2.7 U/ml pyruvate kinase (Sigma), 18 U/ml lactate dehydrogenase (Sigma) and suitable amounts of the sample under investigation. The reaction was performed at 28°C, started by addition of 0.9 mM 2-phosphoglycerate and monitored by recording the decrease in absorbance at 340 nm. One enzyme unit is defined as the amount that catalyses the formation of 1 µmol of phospho*enol*pyruvate/min under the assay conditions.

Polyacrylamide gel electrophoresis and western blotting

SDS–PAGE was carried out as described (39). Rainbow™ High Molecular Weight Marker (Amersham Biosciences) was used as a protein molecular weight marker. Electrophoresis under native conditions was performed as SDS–PAGE except that SDS was omitted in all buffers. Different gel concentrations were employed depending on the experimental requirements, including gradient gels, as specified. High Molecular Weight Calibration Kit (Amersham Biosciences) was used as a protein molecular weight marker. For immunological

detection of proteins, slab gels were blotted onto a polyvinylidene difluoride (PVDF) sheet (40). Immunoreactive bands were revealed using ECL western blotting reagent (Amersham Pharmacia Biotech). Polyclonal anti-PNPase antibodies were raised by rabbit immunization with electrophoretically homogenous PNPase. Antibodies anti-RNase E, anti-enolase and anti-RhlB were kindly provided by A. J. Carpousis.

PNPase cross-linking

PNPase was cross-linked as described by Davies and Stark (41). Enzyme and dimethyl suberimidate were incubated for 6 h at room temperature in 0.2 M triethanolamine hydrochloride (pH 8.5) at concentrations of 0.4 and 4 mg/ml, respectively. As a control, PNPase was also incubated in the absence of the cross-linker and otherwise under the same conditions. After the treatment, 10-μg enzyme samples were subjected to SDS–PAGE and protein revealed by GelCode® Blue Stain Reagent (Pierce).

Northern blotting

Bacterial cultures were grown at 37°C in LD broth with aeration up to OD_{600} = 0.8 and shifted at 16°C, as detailed in the caption to Figure 4 legend and by Zangrossi *et al*. (26). RNA extraction, gel electrophoresis, northern blotting, preparation of the ^{32}P-labelled riboprobes and hybridization were performed as described (42).

RNA electrophoretic mobility shift and filter binding assays

^{32}P-labelled PNP-A riboprobe for RNA-binding assays was synthesized by *in vitro* transcription with T7 RNA polymerase and [α-^{32}P]CTP of a DNA template obtained by PCR amplification of plasmid pAZ8 (29) with oligonucleotides 676 [*CTAATACGACTCACTATAGGG*ATGAATGATCTTCCGTTGC, T7 promoter (43) in italics] and 678 (CAGCGGCAGTAGCCTGACGAGC). The probe corresponded to the first 249 nt of the non-processed *pnp* transcript from the P2 promoter region (DDBJ/EMBL/GenBank accession no. AE000397 coordinates 7949–7701). Then, 0.5 fmol of probe was incubated for 20 min at 21°C in Binding Buffer [50 mM Tris–HCl pH 7.4, 50 mM NaCl, 0.5 mM DTT, 0.025% NP40 (Fluka), 10% glycerol] with increasing amounts of purified PNPase in a final volume of 10 μl. For gel retardation experiments the samples were run in a 5% native polyacrylamide gel electrophoresis at 200 V for 3 h at 4°C. The gel was then dried and analysed by phosphorimaging. The amount of unbound probe was estimated using ImageQuant (Molecular Dynamics) software. For filter binding assays the samples were vacuum filtered at constant flow rate through nitrocellulose filters (Millipore HA 0.45 μm) pre-equilibrated with 1 ml of washing buffer (50 mM Tris–HCl pH 7.4, 50 mM NaCl, 10% glycerol). The filters were then washed with 1 ml of the same buffer and the radioactivity retained was determined by Cerenkov counting in a β-scintillation counter. The dissociation constant K_d was estimated as the PNPase concentration binding half the maximum amount of RNA bound at the highest PNPase concentration. The reported PNPase molar concentrations are referred to the trimeric enzyme.

RESULTS

PNPase from the *pnp-701* mutant has a G454D substitution

To identify the mutation in the *pnp bfl-1* mutant allele, henceforth renamed *pnp-701*, we sequenced the 2.79 kb DNA insert of pAZ12, which had been obtained by PCR amplification of the mutant gene (29). We found only two base changes in the corresponding region in the GenBank AE000397 sequence. To rule out the possibility that these changes were introduced by PCR amplification, we directly sequenced the regions containing the mutations using both wild-type and *pnp-701* genomic DNA as templates. The G7898A base change, which lies upstream of the *pnp* promoter, was found in both the wild-type and the *pnp-701* strains, and thus it likely represents a polymorphism of the *E.coli* C strain. The C6431T base change was found only in *pnp-701* (data not shown); such a mutation causes a glycine to aspartate substitution at amino acid 454 (G454D; PNPase coordinates as in Swiss-Prot accession no. P05055), an evolutionarily conserved Gly residue in most PNPases.

The Pnp-701 homotrimer has an abnormal electrophoretic mobility

In the three-dimensional structure of *S.antibioticus* PNPase, the homologue of Gly454 is a conserved glycine (G478) located at the end of an α-helix (Fig. 1) thought to be important for proper orientation of the trimerization interface (6,44). [In Fig. 5 of Symmons *et al*. (6) this residue has been mistakenly labelled as being directly involved in trimerization contacts (M. F. Symmons, personal communication). Also notice that in the above reference *E.coli* PNPase is translated from an open reading frame starting 23 triplets upstream of the genuine UUG start codon (5) and is thus labelled with different coordinates]. To test whether the *pnp-701* mutation could affect the tertiary and/or quaternary structure of PNPase we analysed the purified PNPase by native gradient gel electrophoresis and visualized the protein by western blotting. The wild-type PNPase migrated as expected for a globular protein of ~200 kDa, compatible with the PNPase homotrimeric structure, whereas the mutant migrated significantly more slowly (Fig. 2A). On the contrary, in denaturing SDS–PAGE, both wild-type and mutant PNPase migrated as single bands of the same apparent molecular weight (see Fig. 2C, lower panel).

To test whether this was caused by an abnormal quaternary structure (either homo- or heteromultimerization) of the mutant PNPase, we cross-linked the purified PNPase with dimethyl suberimidate (4,41) and analysed the products by SDS–PAGE. As shown in Figure 2B, both wild-type and mutant PNPase gave the monomeric and trimeric bands, and no other higher molecular weight complex could be detected, suggesting that the slower migration in non-denaturing gel of Pnp-701 should be imputed to differences in either conformation or electric charge caused by the Gly–Asp mutation. To discriminate between these two possibilities we substituted by *in vitro* site-specific mutagenesis Gly454 with either the polar asparagine or the non-polar leucine (mutants *pnp-702* and *pnp-703*, respectively). Western blot analysis showed that both G454N and G454L PNPase migrated as slowly as the

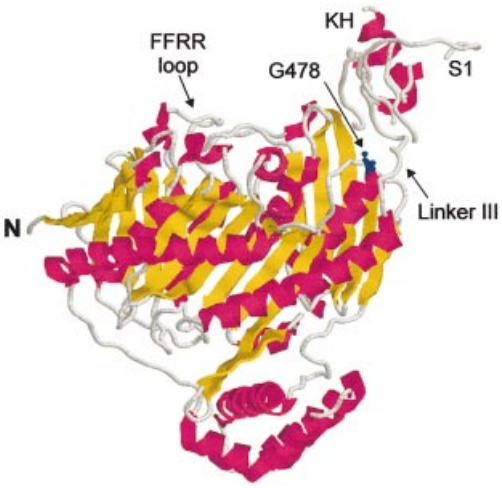

Figure 1. Structure of a PNPase monomer. The cartoon of the tridimensional structure (front view, with trimerization interfaces on the back) of *S.antibioticus* PNPase (GpsI) polypeptide (Protein Data Bank 1E3P) was obtained using RASMOL software (57). The KH and S1 domains have been only partially resolved (6). α-helices are coloured magenta, β-sheets yellow and turns pale blue. G478 (homologous to G454 in *E.coli*) is represented by balls and sticks (blue). H362 (homologous to H338) is located just behind G478 from this perspective.

G454D mutant in non-denaturing gel electrophoresis, whereas no migration differences were observed in SDS–PAGE (Fig. 2C). It should be noted that neither material corresponding to PNPase monomers nor a smear of the main band was detectable in native gradient gel electrophoresis (data not shown), suggesting that mutations in Gly454 do not impair PNPase trimerization.

The G454D mutation does not impair the catalytic properties of PNPase

To compare the catalytic properties of wild-type and mutant PNPase, pure enzymes were assayed for phosphorolytic and polymerase activities. No major differences were detected in either assay, using phosphate and ADP concentrations in the physiological range (Table 1 and Fig. 3). In agreement with previous data (11), in the phosphorolytic assay (Table 1) we assessed a K_m value for phosphate of roughly 1 mM for both enzyme forms, irrespective of poly(A) concentration. Likewise, Pnp-701 polymerasic activity was not impaired by the mutation (Fig. 3). The mutant enzyme did not show the initial lag observed with the wild-type protein. Lag variability among different PNPase preparations has been reported and imputed to trace amounts of contaminating oligonucleotides that stimulate both elongation and *de novo* polymerization (11). In all our PNPase preparations, including those used for these assays, the level of nucleic acid contamination appeared to be rather constant, as assessed by OD_{280}/OD_{260} ratios (0.8 ± 0.06). However, we did not investigate possible differences in length and composition of the contaminants, and thus cannot rule out that the lack of lag is due to differential contamination in enzyme preparations.

The *pnp-701* mutant is defective in autogenous regulation

In an initial characterization of the mutant we surprisingly found ~3-fold higher phosphorolytic activity in crude extracts of the *pnp-701* strain C-5601 than in the wild-type C-5602. Western blot analysis performed using anti-PNPase antibodies showed that the mutant expressed PNPase at a higher level than the parental strain (data not shown; see also Table 2, row 1, and Fig. 2C, but notice that in the latter PNPase is expressed from a plasmid). These data suggest that *pnp-701* could be defective in autogenous regulation.

Alleviation of PNPase autogenous regulation by either mutations or cold shock leads to increased abundance of *pnp* mRNAs, mostly imputable to stabilization of the transcript (22,24,26,27,45). To test whether the higher level of PNPase present in the *pnp-701* mutant could be related to a defect in control of *pnp* mRNA abundance we compared the *pnp* transcript profile of RNA extracted from exponential cultures of *pnp-701* and wild-type cells both at 37°C and at different times after temperature downshift to 16°C. The results of northern blot hybridization analysis using a riboprobe specific for a region at the 5′-end of the *pnp* coding sequence are reported in Figure 4A. The wild-type mRNA profile has been previously described (26,46). All transcripts start at the RNase III processing site and extend to different lengths downstream. The 2.25 kb RNA is a *pnp* monocistronic transcript terminating immediately downstream of the *pnp* coding region. This form appears to be produced in a PNPase-dependent manner by processing of the longer RNA species, as it is not detected in a PNPase nonsense mutant (26). The 2.5 kb (monocistronic) and 3.3 kb (bicistronic) forms end, respectively, within the two genes *nlpI* and *deaD* immediately downstream, whereas the 5.4 kb transcript is a polycistronic *pnp-nlpI-deaD* message. The transcription profile of the *pnp-701* mutant differed in several respects from the wild type.

Overall, the monocistronic (2.25 and 2.5 kb) *pnp* mRNA signals at 37°C were much stronger in the mutant (Fig. 4A, lanes 0). A 10-fold longer exposure of the wild-type RNA blot was required to obtain a signal comparable to that of the mutant (data not shown).

The relative abundance of the 2.5 kb transcript was higher in the mutant, where the 2.5 and 2.25 kb forms exhibited comparable intensities. These facts could be imputed to an increased stability of the monocistronic *pnp* mRNAs in *pnp-701* (see below).

Immediately after cold shock the signals of the monocistronic (2.5 and 2.25) *pnp* mRNAs did not significantly increase further in *pnp-701*, in contrast with the sharp increase in wild-type cells. A small increase could be observed in the mutant late after temperature downshift, when the wild-type *pnp* mRNA returned to a pre-cold shock level. These observations suggest that in the mutant autogenous control at 37°C is alleviated to the same extent as in the wild type during cold acclimation.

Induction of the 5.4 and 3.3 kb transcripts, which is thought to occur upon cold shock by transcription antitermination (26,47), was observed in both the wild type and the mutant. However, these transcripts, in particular the 3.3 kb form, persisted longer in the mutant.

To confirm that the higher abundance of the mutant *pnp* transcripts at 37°C depended on increased mRNA stability, we compared the relative stability of wild-type and mutant *pnp* mRNAs by rifampicin–chase analysis. As shown in Figure 4B, the half-life of the mutant *pnp* mRNA was >4 min, whereas in the wild type it was significantly below 2 min, in agreement

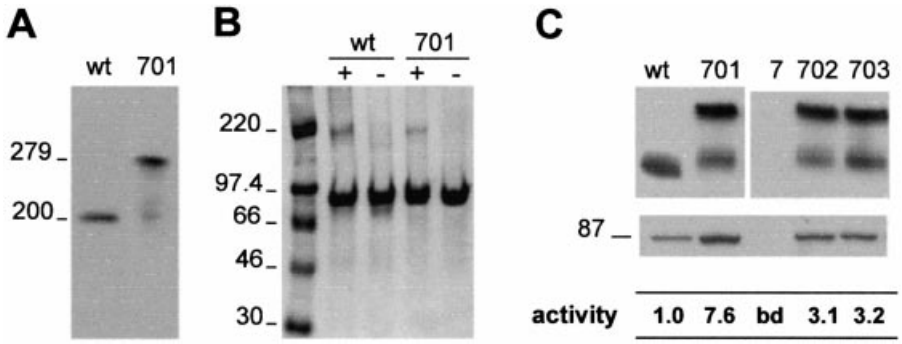

Figure 2. Altered electrophoretic pattern of Pnp-701. (**A**) Native gradient gel electrophoresis. One microgram of purified PNPase from strains C-5602/pAZ101 (*pnp*$^+$) or C-5601/pAZ12 (*pnp-701*) was fractionated by native gradient gel electrophoresis. Immunological detection of the enzyme was performed using anti-PNPase polyclonal antibodies and ECL detection. Molecular weights of protein markers are indicated on the left. (**B**) PNPase cross-linking by dimethyl suberimidate. Ten micrograms of purified Pnp$^+$ or Pnp-701 was incubated in the presence (+) or absence (–) of the DMS cross-linker and run in SDS–PAGE. Proteins were revealed by Gel-Code staining. The molecular weight of the protein markers (first lane) is given on the left. (**C**) Electrophoretic mobility and enzymatic activity of mutant PNPase. Cultures of C-5612 harbouring pAZ8 (wt), pAZ12 (*pnp-701*), pAZ130 (*pnp-702*), pAZ131 (*pnp-703*) or pAZ13 (*pnp-7*, negative control) plasmids were grown at 37°C up to OD_{600} = 0.8. Two micrograms of crude extracts and 0.02 OD_{600} units of cell culture, resuspended and boiled in cracking buffer, were run in native (upper panel) and denaturing acrylamide (lower panel) gel electrophoresis, respectively. Immunodetection of western blots was performed using anti-PNPase antibodies by ECL. Phosphorolytic activity, reported at the bottom as compared with the wild type, was assayed on extracts of the same cultures, as described (36). bd, below detection.

Table 1. Phosphorolytic activity of pure PNPase from *E.coli pnp*$^+$ and *pnp-701*[a]

Poly (A) (μg/ml)	Phosphate (mM)	Specific activity[b] (U/mg protein) Pnp$^+$	Pnp-701
5	1	2.6	2.5
5	10	5.1	4.3
100	1	2.7	2.6
100	10	5.5	5.0

[a]PNPase was purified from strains C-5602/pAZ101 and C-5601/pAZ12.
[b]Determined by the pyruvate kinase/lactate dehydrogenase method as described in Materials and Methods. The average of two independent assays is reported. Standard deviation was <5% of the average.

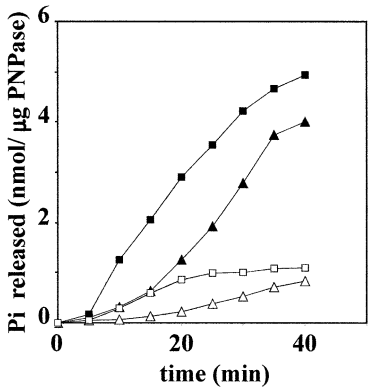

Figure 3. ADP polymerization activity of Pnp-701. Eight micrograms of pure PNPase from strains *pnp*$^+$ (triangles) and *pnp-701* (squares) was incubated at 37°C and pH 7.4 in the presence of 0.2 mM (open symbols) or 1 mM (closed symbols) ADP. The activity was detected by determination of the phosphate released at the indicated times and expressed as nanomoles of phosphate per microgram of PNPase. For other details, see Materials and Methods.

with previous estimates of ~1.5 min (48). Thus it appears that the increased level of PNPase and *pnp* mRNA in the mutant mainly, if not exclusively, depends on the loss of autogenous regulation at the level of mRNA stability.

Pnp-701 is defective in RNA binding

The above results and previously published data (29) suggest that the *pnp-701* mutation affects normal decay and/or maturation of specific messages without significantly impairing the phosphorolytic and polymerasic activities of the enzyme. It is conceivable that the mutation may affect PNPase–RNA interaction, although the mutation is not located in the predicted KH and S1 RNA-binding domains of the protein. To test this idea we performed an RNA electrophoretic mobility shift assay with purified wild-type or mutant PNPase and the untranslated *pnp* leader region as the RNA probe. As shown in Figure 5A, wild-type PNPase caused a complex pattern of RNA probe mobility shifts. At the lowest PNPase concentration (0.05 nM) several shifted bands appeared in the high-mobility range (indicated by bracket I). Supershifted bands in the low-mobility range (bracket II) were formed at 0.8–5 nM, whereas at the highest concentrations (up to 30 nM) most radioactivity did not enter the gel or formed a smear. No unbound probe could be detected starting at 0.3 nM PNPase. On the contrary, RNA binding by Pnp-701 was severely impaired; unbound probe could be found up to 12 nM PNPase, and the supershifted bands in the low-mobility range (complex II) did not appear even at the highest concentration. In agreement with the electrophoretic mobility of PNPase in non-denaturing gels, the shifted bands in complex I were slightly more retarded with the mutant than with the wild-type protein. Similar results were obtained with other different RNA probes including poly(A) (data not shown). The RNA-binding defect of Pnp-701 was confirmed by filter binding assays as shown in Figure 5B. The apparent dissociation constants K_d calculated from filter binding data for Pnp$^+$ and Pnp-701 proteins were 0.3 nM and 1.2 nM, respectively. Although these values represent a rough assessment of PNPase–RNA affinity in that occurrence of multiple binding

Table 2. Degradosome purification from *E.coli pnp*$^+$ and *pnp-701*[a]

Fraction	*pnp*$^+$ Total units		*pnp-701* Total units	
	PNPase[b]	Enolase	PNPase	Enolase
Crude extract	1101	319	2631	321
$(NH_4)_2SO_4$ supernatant	588	305	754	294
$(NH_4)_2SO_4$ pellet	790	35.2	1610	39.3
SP-Sepharose[c]				
Flow through	0	4	660	5.2
50 mM NaCl	143	0.18	172	0.18
300 mM NaCl	21.5	0.15	70.4	0.66
1 M NaCl	497	29.9	485	28.3

[a]From 5 g of C-5602 and C-5601 cells, as described in Materials and Methods.
[b]PNPase activity was determined using the photometric cyclic assay (36).
[c]The column was loaded with the resuspended $(NH4)_2SO_4$ pellets.

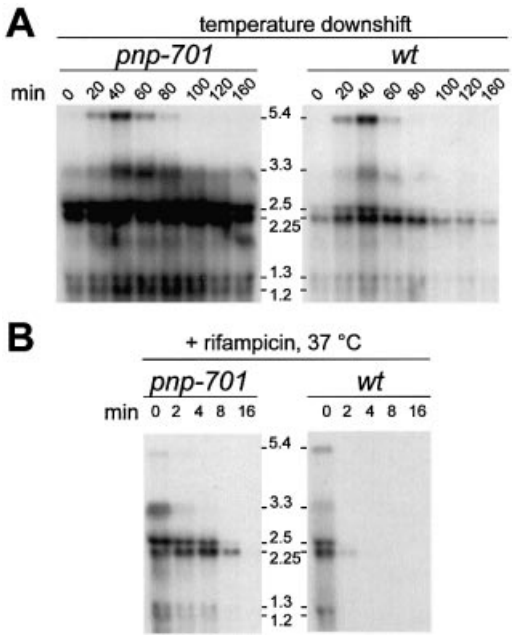

Figure 4. Transcription analysis of the *pnp* operon. (**A**) Cultures of C-5601 (*pnp-701*, left panel) and C-5602 (*pnp*$^+$, right panel) were grown in LD at 37°C with aeration up to OD_{600} = 0.8 (~1.0–1.2 × 10^8 cells ml^{-1}) and quickly transferred at 16°C. Aliquots were sampled immediately before (0) and at different times after the temperature downshift (indicated in minutes above the lanes). RNA was extracted, resolved by 1.5% agarose gel electrophoresis and analysed by northern blot hybridization with the radiolabelled riboprobe pAZ016. The size of the RNAs (in kb) is indicated in the middle. (**B**) Stability of *pnp* transcripts. Cultures of C-5601 (*pnp-701*, left panel) and C-5602 (*pnp*$^+$, right panel) were grown in LD at 37°C with aeration up to OD_{600} = 0.8 (~1.0–1.2 × 10^8 cells ml^{-1}), rifampicin (400 μg/ml) was added and incubation continued at the same temperature. Aliquots were sampled at different times after rifampicin treatment; RNA was extracted and northern blotted as described in (A).

events is disregarded, they nevertheless provide a quantitative estimate of the significant decrease in RNA affinity caused by the mutation. Moreover, it should be noted in Figure 5B that Pnp-701 exhibited not only a higher apparent K_d, but also a lower capacity (~60% of wild type) to bind the RNA probe at the highest protein concentration tested.

Pnp-701 is loosely associated with the RNA degradosome

We also characterized the consequences of the G454D mutation on PNPase assembly into the RNA degradosome. The complex was purified from wild and mutant *E.coli* strains C-5602 and C-5601 essentially as described by Carpousis *et al.* (16) by ammonium sulphate precipitation and SP-Sepharose chromatography. PNPase and enolase activities measured at the different purification steps are reported in Table 2. It may be noted that PNPase activities from the mutant strain in both crude extracts and ammonium sulphate precipitate were ~2.5-fold more abundant than in the wild-type preparations, in contrast with the almost equal enolase activities detected in the two strains under the same conditions. However, only PNPase from *pnp*$^+$ was entirely bound to the SP-Sepharose column, whereas more than 50% of the mutant enzyme was found in the flowthrough, suggesting that a significant fraction of Pnp-701 was not associated with the RNA degradosome. As a result, the amounts of PNPase and enolase in the purified degradosome, which is eluted from the column with 1 M NaCl buffer, were very similar in the two strains, suggesting a similar composition of the complex bound to SP-Sepharose.

We then analysed the SP-Sepharose purified material by FPLC on a Superose 6 HR 10/30 column so as to compare the aggregation states of the wild-type and mutant complexes. Fractions obtained from gel filtration were assayed for PNPase and enolase activities as well as for the presence of the degradosome components by western blotting with antibodies against PNPase, enolase, RhlB and RNase E. The results are shown in Figure 6. PNPase and enolase from wild-type degradosome co-eluted in a major peak at an apparent molecular weight of 2170 kDa. Western blotting of these fractions showed, in addition, the presence of RNase E and RhlB helicase. A minor peak at ~560 kDa contained essentially PNPase and enolase, whereas RNase E and RhlB could not be detected by western blotting. The tail fractions contained PNPase only, in a molecular weight region consistent with the elution of the PNPase homotrimer. These data suggest that the RNA degradosome purified according to the above procedure is mostly a high molecular weight aggregate, and that only a small fraction of PNPase may dissociate from the degradosome at any step after low-salt washes on SP-Sepharose. On the contrary, most PNPase and enolase from the mutant degradosome did not co-elute in gel filtration. The major peak of enolase was eluted at ~1215 kDa together with RNase E and PNPase, whereas the major peak of PNPase was eluted at ⩽235 kDa and did not contain other degradosome components. An intermediate peak at 435 kDa contained both PNPase and enolase, with trace amounts of RNase E. Unfortunately, we were unable to detect RhlB by western blotting in the gel filtration fractions, although the protein was present in the SP-Sepharose purified material. This appears to be due to the low sensitivity and specificity of the available antibodies; probably RhlB was spread in several fractions in amounts below detectability. These data suggest that the RNA degradosome from *E.coli pnp-701* mutant bound to the SP-Sepharose column was prone to dissociate at some subsequent purification step, indicating that the mutant PNPase was more loosely associated to the degradosome than the wild type.

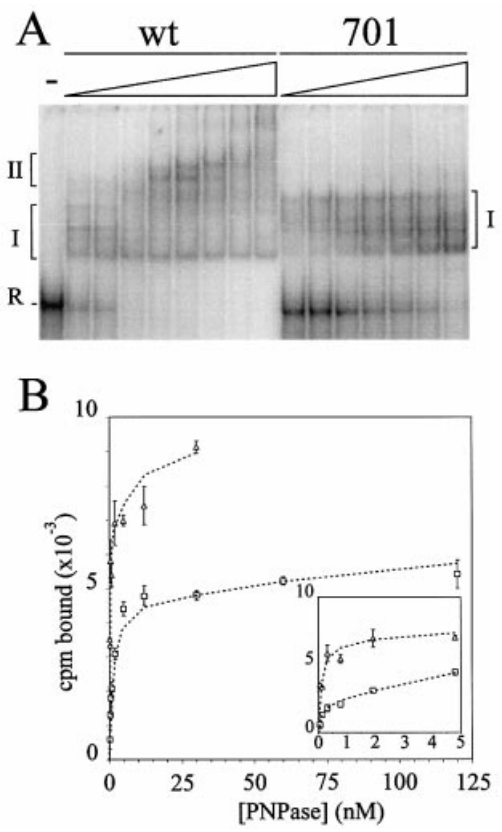

Figure 5. PNPase–RNA-binding assays. (**A**) Electrophoretic mobility shift assays. The radiolabelled PNP-A RNA probe (0.05 nM) without (first lane) and with increasing amounts of PNPase was incubated for 20 min at 21°C and run in 5% polyacrylamide gel. Pnp$^+$ and Pnp-701 were added from 0.05 to 30 nM and 0.12 to 30 nM, respectively, at 2.5× increments. The autoradiographic image was obtained by phosphorimaging. No degradation bands were detectable below the full-length RNA. (**B**) Duplicate samples, prepared as described for (A), were filtered through nitrocellulose membranes and the radioactivity retained by the filters was measured, as described in Materials and Methods, and plotted versus PNPase concentration. Triangles, Pnp$^+$; squares, Pnp-701. In the inset, a blow-out of the PNPase low concentration points is shown.

DISCUSSION

Structural defect of Pnp-701

Pnp-701 has an aspartate substitution at the evolutionarily conserved Gly454 residue. Assuming that the *E.coli* PNPase three-dimensional structure may be superimposed on that of its *S.antibioticus* homologue, the mutated Gly454 locates at the end of an α-helix thought to be important for proper orientation of the trimerization interface; in addition, this conserved residue may contribute to the correct placing of the linker III which positions the KH domain on the upper surface of the enzyme (6,44) (see Fig. 1). Moreover, from the partial modelling of this region, it appears that the S1 domain might make a contact with this residue.

We have shown that the substitution of Gly454 with any bulkier amino acid (Asp, Asn and Leu) leads to an altered electrophoretic mobility in non-denaturing gel electrophoresis, irrespective of the hydropathicity of its lateral chain. Therefore it appears that the delay in electrophoretic mobility is not directly caused by the charge of the substituting amino acid. We suggest that these mutations may change the conformation of the PNPase subunit, possibly by distorting the orientation of the trimerization interface (without impeding trimerization) and/or the positioning of the KH and S1 domains. The final geometry of the trimer could thus be altered (it could possibly be less compact), as indicated by the electrophoretic mobility of the mutant protein. It appears from our *in vitro* experiments that such a structural change in *pnp-701*, the more extensively characterized of the mutants, does not significantly affect either phosphorolytic or polymerasic activities whereas it seems to affect RNA binding and stability of degradosome association.

RNA binding

PNPase seems to bind ssRNA without any apparent sequence specificity (13, this work). Pioneering work (10,11,49) led to the proposal that PNPase has two groups of RNA-binding subsites: a first group, with a short residence time, at the catalytic site(s), and a second region with a long residence time. Supposedly, the former would bind at the 3′-end whereas the latter would bind at the 5′-end of and/or internally to the RNA molecule. This idea was further supported by electron micrographic observations (50,51) and by identification of the KH and S1 RNA-binding domains at the C-terminus of PNPase (5,6,52), which provided a rationale for the observation that a proteolytic fragment of PNPase still retained enzymatic activity (10,53). It has since been commonly assumed that the KH and S1 domains are responsible for the internal RNA binding. In agreement with this idea, mutations affecting either or both KH and S1 may disrupt PNPase autogenous control, which is believed to require both phosphorolytic activity and PNPase–RNA interactions, without substantially impairing the catalytic activities of the enzyme (24,25).

Pnp-701 is defective in RNA binding and exhibits a higher K_d and a decreased capacity for RNA. Interestingly, the mutation maps outside the putative RNA-binding domains KH and S1, suggesting that the mutation may indirectly affect the RNA-binding properties of KH and S1. Alternatively other PNPase domains affected by the mutation participate in RNA binding.

The complex pattern of wild-type PNPase–RNA bands obtained in our electrophoretic mobility shift assays will deserve further investigations. The pattern is in part different from that described previously (13). This may be ascribed to both the different assay conditions and the different probe used. We believe that the increasingly slower bands in complex II appearing at high Pnp$^+$ concentrations (supershifted bands) correlate with the increasing number of PNPase molecules bound to a single RNA probe. By assuming that only one PNPase molecule may be bound to the 3′-end of an RNA molecule, it is implied that supershifted bands contain at least one PNPase molecule bound to RNA internally and/or at the 5′-end. Binding of two PNPases bound at both ends of a single RNA molecule has been documented by electron microscopy (51). On the other hand, the different bands observed at the lowest concentration (complex I) may represent different types of complexes between one molecule of PNPase (at any allowed position on the RNA molecule) and one molecule of RNA in different conformations (secondary

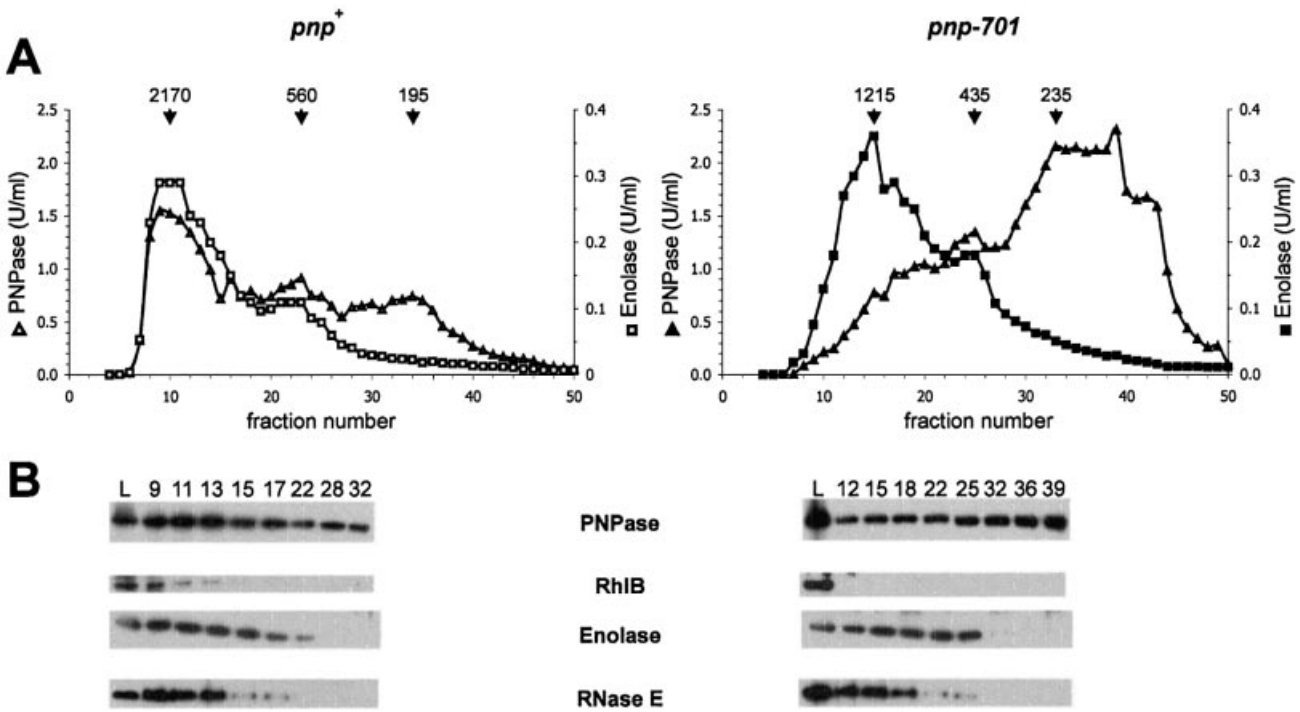

Figure 6. Analysis of the degradosome. (**A**) Gel filtration of partially purified degradosome from *E.coli pnp*+ (left) and *pnp-701* (right) strains. Extracts were enriched in degradosome by ammonium sulphate precipitation and SP-Sepharose chromatography as described (16). Such partially purified preparations (600 µg protein) were then loaded onto a Superose 6 HR 10/30 column pre-equilibrated with 20 mM Tris–HCl pH 7.4, 0.3 M NaCl, 1 mM EDTA, 0.1 mM DTT, 0.1 mM PMSF, 0.1% Genapol X-80 and EDTA-free protease inhibitor. Elution was performed at a flow rate of 0.5 ml/min in the same buffer. Then, 0.25-ml fractions were collected and assayed for enolase and PNPase activity. The molecular mass of relevant peaks is indicated. (**B**) Western blotting of gel filtration fractions: 21 µl of each fraction indicated on top of the lanes or 2 µg of the partially purified degradosome (L) were western blotted using the antibodies against the protein indicated on the left.

structures). This idea is supported by the observation that using either poly(A) or short RNAs (i.e. non-structured RNAs) as probes, complex I appeared as a single band with both wild-type and Pnp-701 proteins (unpublished data). The fastest band in complex I remained at approximately constant intensity at all Pnp+ concentrations, suggesting that a fraction of RNA molecules are in a conformation that cannot bind more that one PNPase. It should be noted that in the conditions of the RNA-binding assay no degradation of the probe could be detected (data not shown), and it is thus implausible that the bands in complex I originate from different lengths of partially degraded RNA.

The lack of complex II supershifted bands with the mutant PNPase suggests that only one protein may be bound per RNA molecule. Since the catalytic abilities of the enzyme are not impaired by the *pnp-701* mutation and require interaction with RNA, it may be suggested that the residual RNA-binding activity of Pnp-701, visualized by complex I, represents the catalytic binding at the 3′-end of the RNA molecule required for phosphorolysis or polymerization and that Pnp-701 may thus be defective in non-catalytic binding.

Pnp-701 association with RNA degradosome

The *pnp-701* mutation also seems to affect the stability of the purified RNA degradosome. Notably, both the composition and the yield of degradosomes from wt or *pnp-701* cells retained by the SP-Sepharose column were comparable. Gel filtration analysis, however, revealed differences in the stability of the two SP-Sepharose purified complexes. The wild-type degradosome eluted in a major peak of >2 MDa containing PNPase, RNase E, RhlB and enolase, and a minor 0.56 MDa peak containing PNPase and enolase. Only a small fraction of PNPase not associated with other degradosome components was eluted in the tail fractions. In contrast, the mutant degradosome recovered from SP-Sepharose seemed to dissociate in lower molecular weight subcomplexes: the largest one (~1.2 MDa) containing PNPase, RNase E and enolase; and a 0.4 MDa complex containing essentially PNPase and enolase. Moreover, most PNPase was no longer associated with other known degradosome components and was eluted in a lower molecular weight tail peak (RhlB was probably diluted out in many fractions and was below detection of the available antibodies). These data suggest that the Pnp-701-containing multienzyme complex is more prone to disaggregation and dissociates upon purification. The mutant degradosome may have dissociated at any step between elution from SP-Sepharose with 1 M salt and gel filtration. Although such instability might be revealed only under non-physiological conditions and might not impair *in vivo* degradosome assembly, it is nevertheless diagnostic of a looser association of Pnp-701 with the RNA degradosome, possibly as a consequence of a structural defect of PNPase.

Control of specific mRNAs stability and/or processing

Current models for PNPase autogenous regulation imply both catalytic activity and RNA binding by PNPase. Evidence

supporting the latter claim have been indirect so far and are mainly based on the observation that mutations affecting either or both KH and S1 may disrupt PNPase autogenous control without substantially impairing its catalytic activities (24,25). However, KH and S1 mutants defective in autogenous regulation have never been tested for RNA binding. Thus the data on Pnp-701 we have presented provide the first experimental evidence of a correlation between RNA binding and autogenous regulation defects.

Likewise, the requirement of phosphorolytic activity for autogenous control has been inferred from the analysis of PNPase mutants impaired in the catalytic properties (24) on the assumption that RNA binding was not affected since such mutations were not located in the KH and S1 domains. However, RNA binding of these mutant PNPases was not measured; on the other hand, we have learned from Pnp-701 that mutations outside of KH and S1 may impair RNA binding. Therefore, whether phosphorolysis is required for PNPase autogenous control remains an open question.

Interestingly, Jarrige *et al.* (24) obtained two PNPase mutants (Pnp-E81K and Pnp-H338G) harbouring mutations at residues not located in the RNA-binding domains that are impaired in autogenous regulation but not in catalytic activities, and might therefore be affected in RNA binding. Residue E81 is located in a flexible FFRR loop that connects the N-terminal trimerization interface and the first core domain, and could also be involved in entrapping the RNA adjacent to the KH domain; H338 is within the C-terminal trimerization interface, below linker III and close to G454. Thus mutations located in the core may alter the precise geometry of the trimeric protein and directly or indirectly affect RNA binding. It may be worth noting that, like Pnp-701, PNPase carrying the H338G mutation migrates more slowly than the wild-type enzyme in native gels, whereas the E81K mutant does not. However, in a screen for PNPase mutants we isolated the E81D and E81L mutations, which affect both autogenous regulation and native gel mobility (unpublished results). Overall, the slower electrophoretic mobility of these mutants suggests that such mutations may modify the geometry of either trimerization interface and/or the correct positioning of the RNA-binding domains, which may result in an abnormal conformation of the trimer. This in turn may interfere with RNA binding either directly or by altering the properties of the KH and S1 domains. It would be interesting to measure the RNA-binding affinity of these and other mutants such as Pnp-702 and Pnp-703 to determine quantitatively whether a correlation between defects in RNA binding and autogenous regulation may be established.

A prerequisite for autogenous control is RNase III processing of *pnp* mRNA untranslated leader (48). It could be possible that PNPase binding to the leader may control efficiency of RNase III processing, e.g. by affecting RNA secondary structure and/or RNase III access to the target. This idea, however, seems implausible since neither by northern blotting (Fig. 4) nor by primer extension (data not shown) could we detect RNase III unprocessed species. Therefore alleviation of autogenous regulation depends on the inability of Pnp-701 to destabilize the RNase III processed RNA, likely because of its defective RNA binding.

The most abundant form of *pnp* monocistronic mRNA present at 37°C in wild-type cells is the 2.25 kb transcript, which extends from the RNase III cut site to the transcription termination point (26,46). Maturation of this mRNA, which appears to derive largely by PNPase-dependent 3′-end degradation of the longer 2.5 kb species (26), is partially affected in *pnp-701*. An intriguing possibility that should be addressed is whether *pnp* mRNA 3′-end maturation, in addition to the proposed PNPase interactions with its 5′-end (21,22), plays a role in autogenous control of PNPase. It should also be observed that the increment of *pnp* mRNA abundance in the mutant is higher than the increment in PNPase. This suggests that a translational control could be operating in addition to the control on *pnp* mRNA stability.

Escherichia coli pnp-701 was isolated as a mutant unable to efficiently support lysogenization by phage P4. In this mutant, the precursors of CI RNA, the P4 immunity factor, were more stable and less efficiently processed by RNase P (29,30), which generates the 5′-end of CI (54,55). By comparison with the phenotype of PNPase-deficient mutants, it was proposed that *pnp-701* was a leaky PNPase mutant, and that PNPase is required to process the 3′-end of the primary transcripts covering the P4 immunity region, thus generating a suitable substrate for RNase P (29,56). The molecular characterization of Pnp-701 indicates that, like destabilization of *pnp* transcript, maturation of P4 CI RNA does not simply require the enzymatic activities of PNPase, but also specific RNA–PNPase interactions that may destabilize the primary transcripts and allow further processing. Whether specific determinants are required on these RNA molecules for PNPase interaction is a matter of current investigation.

ACKNOWLEDGEMENTS

We thank A. J. Carpousis for the gift of antibodies against the different RNA degradosome components, and M. Sana and R. Capizzuto for participating in some stages of this work. F.B. was supported by a postdoctoral fellowship from Università degli Studi di Milano. This research was supported by grants from Ministero dell'Istruzione, dell'Università e della Ricerca (Programmi di Rilevante Interesse Nazionale 1999 and 2001, and FIRB 2001), Rome.

REFERENCES

1. Coburn,G.A. and Mackie,G.A. (1999) Degradation of mRNA in *Escherichia coli*: an old problem with some new twists. *Prog. Nucleic Acid Res. Mol. Biol.*, **62**, 55–108.
2. Schuster,G., Lisitsky,I. and Klaff,P. (1999) Polyadenylation and degradation of mRNA in the chloroplast. *Plant Physiol.*, **120**, 937–944.
3. Piwowarski,J., Grzechnik,P., Dziembowski,A., Dmochowska,A., Minczuk,M. and Stepien,P.P. (2003). Human polynucleotide phosphorylase, hPNPase, is localized in mitochondria. *J. Mol. Biol.*, **329**, 853–857.
4. Portier,C. (1975) Quaternary structure of polynucleotide phosphorylase from *Escherichia coli*: evidence of a complex between two types of polypeptide chains. *Eur. J. Biochem.*, **55**, 573–582.
5. Régnier,P., Grunberg Manago,M. and Portier,C. (1987) Nucleotide sequence of the *pnp* gene of *Escherichia coli* encoding polynucleotide phosphorylase. Homology of the primary structure of the protein with the RNA-binding domain of ribosomal protein S1. *J. Biol. Chem.*, **262**, 63–68.
6. Symmons,M.F., Jones,G.H. and Luisi,B.F. (2000) A duplicated fold is the structural basis for polynucleotide phosphorylase catalytic activity, processivity and regulation. *Structure Fold Des.*, **8**, 1215–1226.

7. Bycroft,M., Hubbard,T.J., Proctor,M., Freund,S.M. and Murzin,A.G. (1997) The solution structure of the S1 RNA binding domain: a member of an ancient nucleic acid-binding fold. *Cell*, **88**, 235–242.
8. Mattaj,I.W. (1993) RNA recognition: a family matter? *Cell*, **73**, 837–840.
9. Thang,M.N., Thang,D.C. and Grunberg Manago,M. (1967) An altered polynucleotide phosphorylase in *E.coli* mutant Q13. *Biochem. Biophys. Res. Commun.*, **28**, 374–379.
10. Godefroy,T. (1970) Kinetics of polymerization and phosphorolysis reactions of *Escherichia coli* polynucleotide phosphorylase. Evidence for multiple binding of polynucleotide in phosphorolysis. *Eur. J. Biochem.*, **14**, 222–231.
11. Godefroy,T., Cohn,M. and Grunberg Manago,M. (1970) Kinetics of polymerization and phosphorolysis reactions of *E.coli* polynucleotide phosphorylase. Role of oligonucleotides in polymerization. *Eur. J. Biochem.*, **12**, 236–249.
12. Chou,J.Y. and Singer,M.F. (1971) Deoxyadenosine diphosphate as a substrate and inhibitor of polynucleotide phosphorylase of *Micrococcus luteus*. 3. Copolymerization of adenosine diphosphate and deoxyadenosine diphosphate. *J. Biol. Chem.*, **246**, 7505–7513.
13. Bermudez Cruz,R.M., García Mena,J. and Montanez,C. (2002) Polynucleotide phosphorylase binds to ssRNA with same affinity as to ssDNA. *Biochimie*, **84**, 321–328.
14. Donovan,W.P. and Kushner,S.R. (1986) Polynucleotide phosphorylase and ribonuclease II are required for cell viability and mRNA turnover in *Escherichia coli* K-12. *Proc. Natl Acad. Sci. USA*, **83**, 120–124.
15. Mohanty,B.K. and Kushner,S.R. (2000) Polynucleotide phosphorylase, RNase II and RNase E play different roles in the *in vivo* modulation of polyadenylation in *Escherichia coli*. *Mol. Microbiol.*, **36**, 982–994.
16. Carpousis,A.J., Van Houwe,G., Ehretsmann,C. and Krisch,H.M. (1994) Copurification of *E.coli* RNase E and PNPase: evidence for a specific association between two enzymes important in RNA processing and degradation. *Cell*, **76**, 889–900.
17. Vanzo,N.F., Li,Y.S., Py,B., Blum,E., Higgins,C.F., Raynard,L.C., Krisch,H.M. and Carpousis,A.J. (1998) Ribonuclease E organizes the protein interactions in the *Escherichia coli* RNA degradosome. *Genes Dev.*, **12**, 2770–2781.
18. Cheng,Z.F., Zuo,Y., Li,Z., Rudd,K.E. and Deutscher,M.P. (1998) The *vacB* gene required for virulence in *Shigella flexneri* and *Escherichia coli* encodes the exoribonuclease RNase R. *J. Biol. Chem.* **273**, 14077–14080.
19. Cheng,Z.F. and Deutscher,M.P. (2003) Quality control of ribosomal RNA mediated by polynucleotide phosphorylase and RNase R. *Proc. Natl Acad. Sci. USA*, **100**, 6388–6393.
20. Luttinger,A., Hahn,J. and Dubnau,D. (1996) Polynucleotide phosphorylase is necessary for competence development in *Bacillus subtilis*. *Mol. Microbiol.*, **19**, 343–356.
21. Robert-LeMeur,M. and Portier,C. (1992) *E.coli* polynucleotide phosphorylase expression is autoregulated through an RNase III-dependent mechanism. *EMBO J.*, **11**, 2633–2641.
22. Robert-LeMeur,M. and Portier,C (1994) Polynucleotide phosphorylase of *Escherichia coli* induces the degradation of its RNase III processed messenger by preventing its translation. *Nucleic Acids Res.*, **22**, 397–403.
23. Jarrige,A.C., Mathy,N. and Portier,C. (2001) PNPase autocontrols its expression by degrading a double-stranded structure in the *pnp* mRNA leader. *EMBO J.*, **20**, 6845–6855.
24. Jarrige,A., Brechemier,B., Mathy,N., Duche,O. and Portier,C. (2002) Mutational analysis of polynucleotide phosphorylase from *Escherichia coli*. *J. Mol. Biol.*, **321**, 397–409.
25. García Mena,J., Das,A., Sanchez-Trujillo,A., Portier,C. and Montanez,C. (1999) A novel mutation in the KH domain of polynucleotide phosphorylase affects autoregulation and mRNA decay in *Escherichia coli*. *Mol. Microbiol.*, **33**, 235–248.
26. Zangrossi,S., Briani,F., Ghisotti,D., Regonesi,M., Tortora,P. and Dehò,G. (2000) Transcriptional and post-transcriptional control of polynucleotide phosphorylase during cold acclimation in *Escherichia coli*. *Mol. Microbiol.* **36**, 1470–1480.
27. Beran,R.K. and Simons,R.W. (2001) Cold-temperature induction of *Escherichia coli* polynucleotide phosphorylase occurs by reversal of its autoregulation. *Mol. Microbiol.*, **39**, 112–125.
28. Mathy,N., Jarrige,A.C., Robert-Le Meur,M. and Portier,C. (2001) Increased expression of *Escherichia coli* polynucleotide phosphorylase at low temperatures is linked to a decrease in the efficiency of autocontrol. *J. Bacteriol.*, **183**, 3848–3854.
29. Piazza,F., Zappone,M., Sana,M., Briani,F. and Dehò,G. (1996) Polynucleotide phosphorylase of *Escherichia coli* is required for the establishment of bacteriophage P4 immunity. *J. Bacteriol.*, **178**, 5513–5521.
30. Briani,F., Forti,F., Ghisotti,D. and Dehò,G. (2001) The plasmid status of satellite bacteriophage P4. *Plasmid*, **45**, 1–17.
31. Sasaki,I. and Bertani,G. (1965) Growth abnormalities in Hfr derivatives of *Escherichia coli* strain C. *J. Gen. Microbiol.*, **40**, 365–376.
32. Lessl,M., Balzer,D., Lurz,R., Waters,V.L., Guiney,D.G. and Lanka,E. (1992) Dissection of IncP conjugative plasmid transfer: definition of the transfer region Tra2 by mobilization of the Tra1 region in trans. *J. Bacteriol.*, **174**, 2493–2500.
33. Ho,S.N., Hunt,H.D., Horton,R.M., Pullen,J.K. and Pease,L.R. (1989) Site-directed mutagenesis by overlap extension using the polymerase chain reaction. *Gene*, **77**, 51–59.
34. Soreq,H. and Littauer,U.Z. (1977) Purification and characterization of polynucleotide phosphorylase from *Escherichia coli*. Probe for the analysis of 3′ sequences of RNA. *J. Biol. Chem.*, **252**, 6885–6888.
35. Nilsson,G., Lundberg,U. and von Gabain,A. (1988) *In vivo* and *in vitro* identity of site specific cleavages in the 5′ non-coding region of *ompA* and *bla* mRNA in *Escherichia coli*. *EMBO J.*, **7**, 2269–2275.
36. Fontanella,L., Pozzuolo,S., Costanzo,A., Favaro,R., Dehò,G. and Tortora,P. (1999) Photometric assay for polynucleotide phosphorylase. *Anal. Biochem.*, **269**, 353–358.
37. Ames,B.N. (1966) Assay of inorganic phosphate, total phosphate and phosphatases. *Methods Enzymol.*, **8**, 115–118.
38. Spring,T.G. and Wold,F. (1975) Enolase from *Escherichia coli*. *Methods Enzymol.*, **42**, 323–329.
39. Laemmli,U.K. (1970) Cleavage of structural proteins during the assembly of the head of bacteriophage T4. *Nature*, **227**, 680–685.
40. Sambrook,J., Fritsch,E.F. and Maniatis,T. (1989) *Molecular Cloning. A Laboratory Manual*. Cold Spring Harbor Laboratory Press, Cold Spring Harbor, NY.
41. Davies,G.E. and Stark,G.R. (1970) Use of dimethyl suberimidate, a cross-linking reagent, in studying the subunit structure of oligomeric proteins. *Proc. Natl Acad. Sci. USA*, **66**, 651–656.
42. Briani,F., Zangrossi,S., Ghisotti,D. and Dehò,G. (1996) A Rho-dependent transcription termination site regulated by bacteriophage P4 RNA immunity factor. *Virology*, **223**, 57–67.
43. Baklanov,M.M., Golikova,L.N. and Malygin,E.G. (1996) Effect on DNA transcription of nucleotide sequences upstream to T7 promoter. *Nucleic Acids Res.*, **24**, 3659–3660.
44. Symmons,M.F., Williams,M.G., Luisi,B.F., Jones,G.H. and Carpousis,A.J. (2002) Running rings around RNA: a superfamily of phosphate-dependent RNases. *Trends Biochem. Sci.*, **27**, 11–18.
45. Régnier,P. and Grunberg Manago,M. (1990) RNase III cleavages in non-coding leaders of *Escherichia coli* transcripts control mRNA stability and genetic expression. *Biochimie*, **72**, 825–834.
46. Régnier,P. and Portier,C. (1986) Initiation, attenuation and RNase III processing of transcripts from the *Escherichia coli* operon encoding ribosomal protein S15 and polynucleotide phosphorylase. *J. Mol. Biol.*, **187**, 23–32.
47. Bae,W., Xia,B., Inouye,M. and Severinov,K. (2000) *Escherichia coli* CspA-family RNA chaperones are transcription antiterminators. *Proc. Natl Acad. Sci. USA*, **97**, 7784–7789.
48. Portier,C., Dondon,L., Grunberg Manago,M. and Régnier,P. (1987) The first step in the functional inactivation of the *Escherichia coli* polynucleotide phosphorylase messenger is a ribonuclease III processing at the 5′ end. *EMBO J.*, **6**, 2165–2170.
49. Thang,M.N., Harvey,R.A. and Grunberg Manago,M. (1970) Model for the elongation of polynucleotide chains by polynucleotide phosphorylase. *J. Mol. Biol.*, **53**, 261–280.
50. Valentine,R.C., Thang,M.N. and Grunberg Manago,M. (1969) Electron microscopy of *Escherichia coli* polynucleotide phosphorylase molecules and polyribonucleotide formation. *J. Mol. Biol.*, **39**, 389–391.
51. Sulewski,M., Marchese-Ragona,S.P., Johnson,K.A. and Benkovic,S.J. (1989) Mechanism of polynucleotide phosphorylase. *Biochemistry*, **28**, 5855–5864.
52. Gibson,T.J., Thompson,J.D. and Heringa,J. (1993) The KH domain occurs in a diverse set of RNA-binding proteins that include the antiterminator NusA and is probably involved in binding to nucleic acid. *FEBS Lett.*, **324**, 361–366.
53. Guissani,A. and Portier,C. (1976) Study on the structure-function relationship of polynucleotide phosphorylase: model of a proteolytic degraded polynucleotide phosphorylase. *Nucleic Acids Res.*, **3**, 3015–3024.

54. Forti,F., Dragoni,I., Briani,F., Dehò,G. and Ghisotti,D. (2002) Characterization of the small antisense CI RNA that regulates bacteriophage P4 immunity. *J. Mol. Biol.*, **315**, 541–549.
55. Forti,F., Sabbattini,P., Sironi,G., Zangrossi,S., Dehò,G. and Ghisotti,D. (1995) *Immunity* determinant of phage-plasmid P4 is a short processed RNA. *J. Mol. Biol.*, **249**, 869–878.
56. Briani,F., Del Vecchio,E., Migliorini,D., Hajnsdorf,E., Régnier,P., Ghisotti,D. and Dehò,G. (2002) RNase E and polyadenyl polymerase I are involved in maturation of CI *RNA*, the P4 phage immunity factor. *J. Mol. Biol.*, **318**, 321–331.
57. Sayle,R.A. and Milner,W. (1995) RASMOL: biomolecular graphics for all. *Trends Biochem. Sci.*, **20**, 374.